Proceedings of the 2001 IEEE/RSJ
International Conference on Intelligent Robots and Systems
Maui, Hawaii, USA, Oct. 29 - Nov. 03, 2001

Optimal Grasping Based on Non-Dimensionalized Performance Indices

Byoung-Ho Kim°,†, Sang-Rok Oh†, Byung-Ju Yi°, and Il Hong Suh°

° : School of Electrical Eng. and Computer Science, Hanyang Univ., Seoul, Korea
† : Intelligent System Control Research Center, KIST, Seoul, Korea
(E-mail: bj@hanyang.ac.kr)

Abstract

When a multi-fingered hand grasps an object, the ways to grasp it stably are infinite, and thus an optimal grasp planning is necessary to find the optimal grasp points for achieving the objective of the given task. For this, we first define several grasp indices to evaluate the quality of each feasible grasp. Since the physical meanings of the defined grasp indices are different from each other, it is not easy to combine those indices to identify the optimal grasping. In this paper, we propose a new generalized grasping performance index to represent all of the grasp indices as one measure based on a non-dimensionalizing technique. Through simulations, we show the trend of the proposed optimal grasp planning is coincident to the physical sense of human grasping.

Keywords : *multi-fingered hand, optimal grasp planning, generalized grasping performance index*

1 Introduction

When a multi-fingered hand grasps an object, the ways to grasp it stably are infinite and thus an optimal grasp planning is required to find the optimal grasp points to satisfy the objective of the given task. In determination of grasp points on object, it is very important to select grasp points in such a way to minimize the grasp error caused by external uncertainties. Even though the selected grasp points are stable, the most stable grasp points are necessary for dextrous manipulation of object.

Many research works have focused on the field of manipulating object grasped by multi-fingered hands[1]-[5]. For dextrous manipulation of object, it is necessary to grasp the most stable points on object. Some researchers tried to find the proper grasp points using some grasp indices[6]-[10]. Li. et al.[6] defined a grasp index which is made up of the singular value of grasp matrix, the volume of wrench space, and the task ellipsoid. They focused optimal grasp points by optimization of the defined grasp index. In this method, the required maximum forces for all directions of each fingertip not only must be known, but also the procedure of computing the defined grasp index is rather complex. Cutkosky[7] defined various analytical grasp indices for grasp modeling and effectively choosing grasp points, and also classified systematic grasp styles considering the grasp geometry and the work characteristics of given task. Through Cutkosky's work, it is known that grasp configuration and manipulability of multi-fingered hands may be different as the grasp styles. Therefore, we can notice that grasp points should be carefully chosen by considering the objective of given task. Park, et al.[8] proposed two different grasp indices, uncertainty grasp index and task compatibility grasp index, where force and velocity transmission ratios are used to consider both the force domain and velocity domain. Since this method is based on hybrid position and force control, the task space must be classified in advance. Thus, the method can be applied to limited cases. In [9], three-fingered grasp synthesis has been studied for polygonal object in two-dimensional space. Here, feasible grasp combinations are sorted as the contact models and force closure grasp based on the object geometry is constructed. Also, grasp search using heuristic function is treated to find the optimal grasp points. In this process of searching the optimal grasp points, the normal directional contact between finger and object is only treated and the heuristic function is dependent upon the limited geometrical condition. So, the method is not easy to extend three-dimensional space and also the manipulable grasp characteristic is not considered yet. In [10][11], optimal grasp points

based on the self-posture changeability of each finger was reported.

In this paper, we propose a method to find the optimal grasp points of the given object with respect to a non-dimensionalized composite grasp index. In section 2, we first define several grasp indices to evaluate the quality of each feasible grasp and then define a non-dimensionalized composite grasp index which combines all of the grasp indices as one measure. In section 3, simulation results show the feasibility of the proposed optimal grasp planning method comparing to the physical sense of human grasping. Also, we discuss the trend of each grasp index as the grasp polygons. Finally, concluding remarks are summarized in section 4.

2 Grasp Index

When a multi-fingered hand grasps an object, contact area of each finger on object can be classified both the feasible contact region(FCR) and the feasible grasp region(FGR). FCR means the kinematically reachable contact region and FGR implies the grasp region considering friction cone. Also, those regions can be detected through visual signal processing[4][16][17].

For stable grasping and manipulation of object, it is very important to select the stable grasp points and then proper hand/arm coordination may be required to guarantee stable manipulation for the given trajectory[1]-[3]. Therefore, an optimal grasp planning is necessary to find the optimal grasp points. Also, since optimal grasp planning problem is associated with the control objective of given task including the geometry of object and the structure of hand[7], task constraints, object constraints, and hand constraints should be simultaneously considered to search the optimal grasp points as shown in Figure 1.

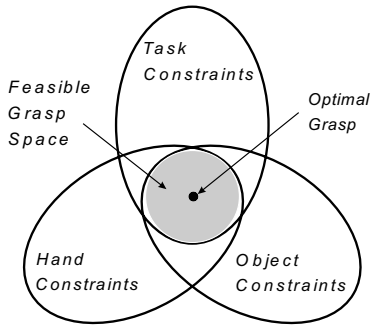

Figure 1: Optimal grasp of multi-fingered hand.

Here, we first define several grasp indices to evaluate the grasp points for optimal grasp. Then, we propose a non-dimensionalized composite grasp index which combines the grasp indices as one measure after normalizing each grasp index. The optimal grasp points in this paper implies the points at which the non-dimensionalized composite grasp index is maximized.

2.1 Stability Grasp Index

The stability grasp index is defined as the quantitative index to evaluate the capability of withstanding external force. For example, consider a L-type object grasped by multi-fingered hand shown in Figure 2.

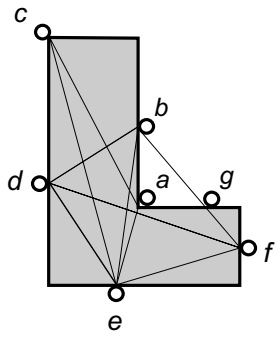

Figure 2: Grasp points for L-type object.

There exists three types of grasp points as shown in Figure 3. In case that a finger grasps the convex vertex of object like Figure 3(b), the finger may be unstable by small external disturbance.

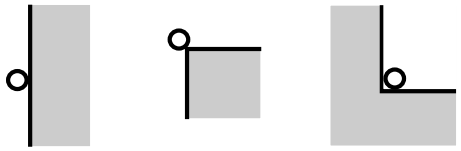

Figure 3: Types of grasp points: (a) edge (b) convex vertex (c) concave vertex.

The concave vertex of Figure 3(c) is not easy to grasp, and also the manipulable range of the finger is limited. Therefore, those points are not adequate as stable and dextrous grasp points. For example, when a three-fingered hand grasps an object shown in Figure 2, grasp polygon ace are more unstable than bde. In this sense, we exclude those points among the candidates of optimal grasp points in advance.

Consider Figure 4 that shows the grasp triangles drawn by connecting the three contact points. The more a grasp triangle forms a regular triangle structure, the more it forms the form closure grasp[9]. Therefore, we can notice that the desired grasp points should be selected to form a regular polygon structure for stable grasp. In this viewpoint, we define the stability grasp index, I_S, as follows:

$$I_S = \frac{1}{\theta_{max}} \sum_{i=1}^{n_f} |\theta_i - \bar{\theta}|, \quad (1)$$

where n_f denotes the number of fingers, and θ_i is the inner angle of the ith grasp point,

$$\bar{\theta} = \frac{180(n_f - 2)}{n_f},$$

and $\bar{\theta}$ denotes the average angle of all inner angles of the grasp polygon and θ_{max} is defined as

$$\begin{aligned} \theta_{max} &= \sum_{i=1}^{n_f} |\theta_i - \bar{\theta}|_{ill\ conditioned} \\ &= (n_f - 2)(180 - \bar{\theta}) + 2\bar{\theta} \end{aligned}$$

which represents the sum of the difference between the inner angle given in the ith grasp point and the average angle when the grasp polygon has the most ill conditioned shape such as line.

Consequently, the stability grasp index is minimized if a grasp polygon has a regular polygon structure.

Note that since the defined stability grasp index only consider the shape of achievable grasp polygons, there exists many polygons of same kind. Thus, another grasp index is necessary to classify more stable grasp points.

2.2 Uncertainty Grasp Index

Even though the grasp polygons bde, bdf, and def in Figure 2 are comparably stable, it is not easy to classify one of them as the most stable grasp polygon. In this case, we can determine better grasp points by estimating the position sensitivity as the location of each grasp point changes. The polygon including the extreme point near the edge may be more unstable. For example, Figure 4(b) is more stable than Figure 4(a). Thus, in order to estimate the position sensitivity of the grasp points, we define the following uncertainty grasp index, given by I_U,

$$I_U = \frac{1}{n_f} \sum_{i=1}^{n_f} {}^i d_e, \quad (2)$$

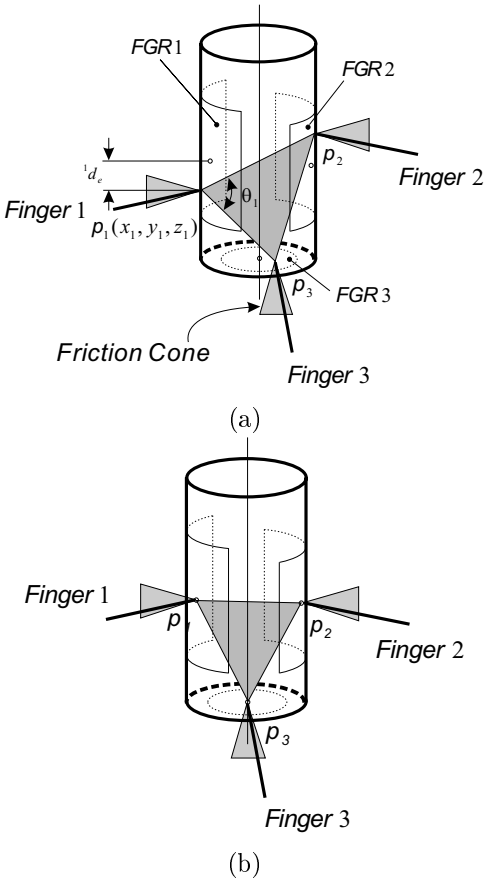

Figure 4: Grasp triangle as grasp location: (a) any point in FGR (b) center point in FGR

where

$${}^i d_e = \sqrt{(x_i - x_{io})^2 + (y_i - y_{io})^2 + (z_i - z_{io})^2},$$

and x_i, y_i, and z_i denote the x-, y-, and z-directional position of the grasp point of the ith finger and x_{io}, y_{io}, and z_{io} denote the center position of FGR in the ith finger, respectively.

Consequently, the uncertainty grasp index is minimized if all fingers grasp the center of feasible grasp regions.

2.3 Maximum Force Transmission Ratio Index

When an object grasped by multi-fingered hands is being manipulated, the force transmission capability of the hand is associated with the grasp geometry of the hand and the configuration of each finger. Thus, for effective manipulation of grasped object, it is reasonable to select the grasp point of each finger in such a way to maximize the force transmission ratio.

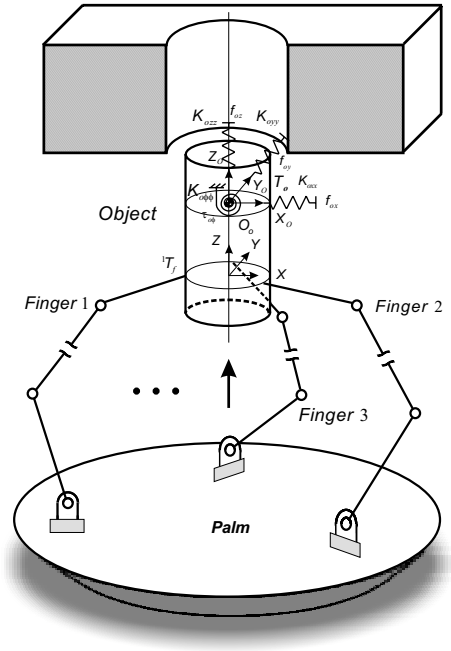

Figure 5: Peg-in-hole task by using multi-fingered hand.

Consider a peg-in-hole task given in Figure 5. The force relation between the operational space and the fingertip space is given by

$$T_o = [\boldsymbol{G}_o^f]^T T_f, \tag{3}$$

where $T_o \in \mathcal{R}^{n\times 1}$ denotes the dynamic forces and moments in the operational space including the inertial load and external load, $T_f \in \mathcal{R}^{m.n_f\times 1}$ fingertip force vector in the fingertip space, and $[\boldsymbol{G}_o^f] \in \mathcal{R}^{m.n_f\times n}$ Jacobian matrix. Here, m denotes the dimension of wrench transmitted through each contact point.

To define the force transmission ratio between the operational space and the fingertip space, we first define the norm of the operational force, $\|T_o\|$, and that of the fingertip space, $\|T_f\|$, as follows:

$$\|T_o\| = \left\{T_o^T T_o\right\}^{\frac{1}{2}}, \tag{4}$$

$$\|T_f\| = \left\{T_f^T T_f\right\}^{\frac{1}{2}}. \tag{5}$$

Substituting (3) into (4), Eq. (4) can be rewritten as

$$\|T_o\| = \left\{T_f^T [\boldsymbol{G}_o^f][\boldsymbol{G}_o^f]^T T_f\right\}^{\frac{1}{2}}. \tag{6}$$

Then, the force transmission ratio between the operational space and the fingertip space is expressed as

$$^o\sigma_F = \frac{\|T_o\|}{\|T_f\|} = \left\{\frac{T_f^T [\boldsymbol{G}_o^f][\boldsymbol{G}_o^f]^T T_f}{T_f^T T_f}\right\}^{\frac{1}{2}}. \tag{7}$$

Based Rayleigh Quotiant[12], the force in the operational space is bounded by

$$^o\sigma_{min}\|T_f\| \le \|T_o\| \le {}^o\sigma_{max}\|T_f\|, \tag{8}$$

where $^o\sigma_{min}$ and $^o\sigma_{max}$ denote the minimum and maximum values of the square root of the singular value of $[\boldsymbol{G}_o^f][\boldsymbol{G}_o^f]^T$, respectively.

Rearranging (8), we have

$$^o\sigma^f_{min}\|T_o\| \le \|T_f\| \le {}^o\sigma^f_{max}\|T_o\|, \tag{9}$$

where

$$^o\sigma^f_{min} = \frac{1}{^o\sigma_{max}}, \tag{10}$$

$$^o\sigma^f_{max} = \frac{1}{^o\sigma_{min}}. \tag{11}$$

and here, $^o\sigma^f_{min}$ and $^o\sigma^f_{max}$ denote the minimum and maximum force transmission ratios between the operational space and the fingertip space, respectively.

It is remarked that if the maximum force transmission ratio is minimized, the resultant load at the fingertip is minimized.

2.4 Task Isotropy Index

When an object is being manipulated by multi-fingered hands, the precise position or force control may not be guaranteed in part if any finger lies near singular position. Isotropy index is useful to measure this configuration. The task isotropy index is defined as

$$\sigma_I^T = \frac{\sigma_{min}^T}{\sigma_{max}^T}, \tag{12}$$

where σ_{min}^T and σ_{max}^T denote the minimum and maximum values of the square root of the singular value of $[\boldsymbol{G}_o^f][\boldsymbol{G}_o^f]^T$, respectively.

Specially, the task isotropy index approaches 1.0 at isotropic configuration and is equal to zero at the singular grasp geometry. Thus, maximizing this index is desirable.

2.5 Stiffness Mapping-Based Grasp Isotropy Index

The stiffness(or compliance) characteristic is fundamental property for various contact tasks. Thus, we

consider the stiffness mapping between the operational space and the fingertip space.

In general, grasping and manipulation of an object grasped by multi-fingered hands is not easy due to the coupling among fingers and/or joints. Recently, an independent finger-based compliance control has been proposed to eliminate the finger coupling effect[13]. The stiffness relation between the operational space and the fingertip space can be expressed as

$$[\boldsymbol{K}_o] = [\boldsymbol{G}_o^f]^T [\boldsymbol{K}_f][\boldsymbol{G}_o^f], \tag{13}$$

where $[\boldsymbol{K}_o]$ and $[\boldsymbol{K}_f]$ denote the desired operational stiffness matrix and the fingertip stiffness matrix, respectively.

An alternative independent stiffness form of (13) can be represented by

$$K_{oo} = [\boldsymbol{B}_f^o]\ K_{ff}, \tag{14}$$

where K_{oo} and K_{ff} denote the independent stiffness elements in the operational and fingertip spaces, respectively. $[\boldsymbol{B}_f^o]$ denotes the stiffness mapping matrix between the operational space and the fingertip space.

It is a function of grasp geometry. To evaluate the quality of the selected grasp points for effective compliant tasks, we define the stiffness mapping-based grasp isotropy index as follows:

$$\sigma_I^S = \frac{\sigma_{min}^S}{\sigma_{max}^S}, \tag{15}$$

where σ_{min}^S and σ_{max}^S denote the minimum and maximum values of the square root of the singular value of $[\boldsymbol{B}_f^o][\boldsymbol{B}_f^o]^T$, respectively.

This index will be very useful for effective peg-in/out-hole tasks shown in Figure 5.

2.6 Non-Dimensionalized Composite Grasp Index

The physical meanings of the defined grasp indices inthe previous sections are different from each other. So, a generalized grasp index is necessary to evaluate a given grasp geometry. Terano, et al.,[14] and Wood[15] proposed a design procedure reflecting fuzzy algorithm. They employ a normalized procedure which rearrange each performance index from 0 to 1 as the task-based preference information.

Now, we define a non-dimensionalized composite grasp index I_{WCG} which evaluates the selected grasp geometry by aggregating all the individual grasp indices as one measure, given by

$$\begin{aligned} I_{WCG} \quad = \quad & min\{(\tilde{I}_S)^{w_1}, (\tilde{I}_U)^{w_2}, (\tilde{I}_{FTR})^{w_3}, \\ & (\tilde{I}_{TASK})^{w_4}, (\tilde{I}_{STIFF})^{w_5}\}, \end{aligned} \tag{16}$$

where $(\tilde{I}_S)^{w_1}$, $(\tilde{I}_U)^{w_2}$, $(\tilde{I}_{FTR})^{w_3}$, $(\tilde{I}_{TASK})^{w_4}$, and $(\tilde{I}_{STIFF})^{w_5}$ denote the normalized stability grasp index, uncertainty grasp index, maximum force transmission ratio index, task isotropy index, and stiffness mapping-based grasp isotropy index, respectively. The weighting factors denoted by $w_i (i = 1, 2, \cdots, 5)$ are set as greater than or equal to 1.0.

Since the stability grasp index, uncertainty grasp index, and maximum force transmission ratio index should be minimized, their normalized indices are defined as

$$\tilde{I}_S = \frac{I_{S,max} - I_S}{I_{S,max} - I_{S,min}}, \tag{17}$$

$$\tilde{I}_U = \frac{I_{U,max} - I_U}{I_{U,max} - I_{U,min}}, \tag{18}$$

and

$$\tilde{I}_{FTR} = \frac{\{{}^o\sigma_{max}^f\}_{max} - {}^o\sigma_{max}^f}{\{{}^o\sigma_{max}^f\}_{max} - \{{}^o\sigma_{max}^f\}_{min}}. \tag{19}$$

On the other hand, the task iostropy index and the stiffness mapping-based grasp index should be maximized. Thus, those normalized indices can be obtained as follows, respectively,

$$\tilde{I}_{TASK} = \frac{\sigma_I^T - \{\sigma_I^T\}_{min}}{\{\sigma_I^T\}_{max} - \{\sigma_I^T\}_{min}}, \tag{20}$$

and

$$\tilde{I}_{STIFF} = \frac{\sigma_I^S - \{\sigma_I^S\}_{min}}{\{\sigma_I^S\}_{max} - \{\sigma_I^S\}_{min}}. \tag{21}$$

Then, we develop the data base of the non-dimensionalized composite grasp index by selecting the minimum values of all normalized grasp indices for each grasp points. Finally, we can choose the optimal grasp points by choosing the largest non-dimensionalized composite grasp index in the data base.

3 Simulation Results

In this section, simulations are performed to show the feasibility of the proposed grasp index. Consider a two-dimensional assembly task using three-fingered hand. The grasp range of each finger is indicated in Table1, where the x- and y-directional coordinates denote the distances from the operational space to the fingertip space in Figure 5.

In the first simulation, we search the optimal grasp points for a peg-in-hole task shown in Figure 5 and

Table 1: Grasp region of each finger(unit: m)

Finger	x-axis		y-axis		Ref.
	initial	end	initial	end	
1	−0.03	−0.03	−0.07	−0.03	Fig. 5
2	0.03	0.03	−0.07	−0.04	Fig. 7
3	−0.02	−0.02	−0.1	−0.1	

also, we discuss the trend of the proposed grasp indices. In this simulation, 11 grasp points for each finger are chosen as the candidates of the optimal grasp points, and the weighting factors $w_i (i = 1, \cdots, 5)$ are set as 1.0, 1.5, 1.0, 1.0, 1.0, respectively. To be specific, the weighting factor of the uncertainty grasp index is set relatively greater than the others. When the feasible grasp region for each finger is given by Figure 7, the non-dimensionalized composite grasp indices for all achievable grasp points can be shown in Figure 8.

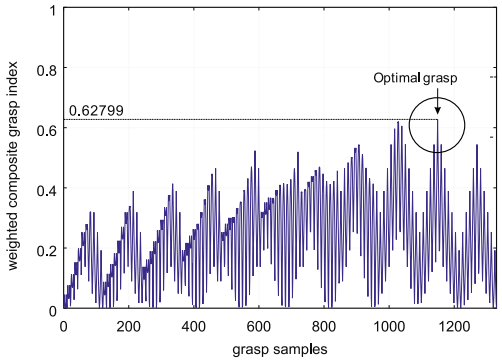

Figure 6: Non-dimensionalized composite grasp index for all grasp points.

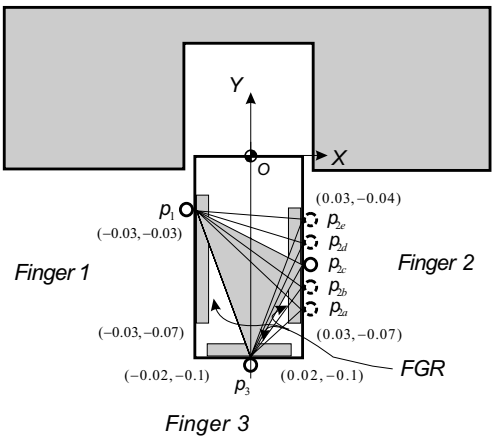

Figure 7: Grasp points and polygons.

From Figure 6, we can confirm that the 1149th grasp sample point is the optimal grasp point.

Now, to discuss the trend of the proposed grasp indices, consider the optimal grasp polygon and the neighborhood of optimal point. Table 2 presents the evaluated non-dimensionalized composite grasp indices for several grasp polygons, where the positions(x, y) of fingers 1 and 3 are (−0.03,−0.034) and (0.0,−0.1), respectively.

Table2: Evaluatednon-dimensionalized grasp index for each grasp polygon

Grasp polygon	pos. of finger 2 (x,y)[m]	I_{WCG}	Remarks
$p_1 p_{2a} p_3$	0.03,−0.061	0.465	Fig. 7
$p_1 p_{2b} p_3$	0.03,−0.058	0.544	
$p_1 p_{2c} p_3$	0.03,−0.055	0.628	
$p_1 p_{2d} p_3$	0.03,−0.052	0.544	
$p_1 p_{2e} p_3$	0.03,−0.049	0.465	

From Table 2, we can notice that $p_1 p_{2c} p_3$ is selected as the optimal grasp polygon which is coincident to intuition. Also, note that the non-dimensionalized composite grasp index of the grasp polygon $p_1 p_{2a} p_3$ is the same as that of the grasp polygon $p_1 p_{2e} p_3$. However, even though the non-dimensionalized composite grasp indices are identical, the individual grasp index may differ from each other. The normalized grasp indices for the grasp polygons are illustrated in Table 3.

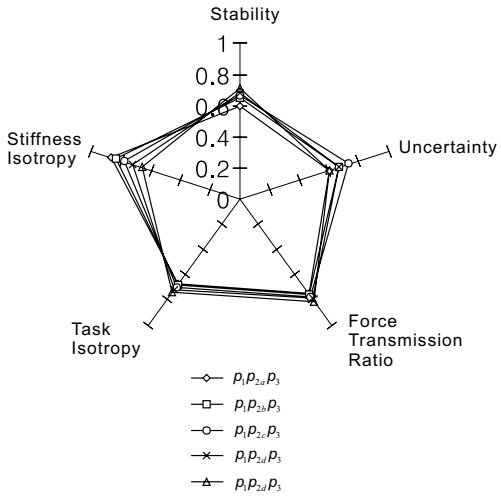

Figure 8: Normalized grasp indices as the grasp points.

From Figure 8 and Table 3, we can observe that the stiffness isotropy is the largest in the grasp polygon

Table 3: Normalized grasp indices for each grasp polygon

Grasp polygon	$\tilde{I}_S$	$\tilde{I}_U$	$\tilde{I}_{FTR}$	$\tilde{I}_{TASK}$	$\tilde{I}_{STIFF}$
$p_1p_{2a}p_3$	0.594	0.600	0.746	0.671	0.868
$p_1p_{2b}p_3$	0.647	0.667	0.755	0.683	0.831
$p_1p_{2c}p_3$	0.662	0.733	0.769	0.698	0.782
$p_1p_{2d}p_3$	0.682	0.667	0.785	0.718	0.723
$p_1p_{2e}p_3$	0.708	0.600	0.805	0.743	0.658

$p_1p_{2a}p_3$, and the grasp polygon $p_1p_{2c}p_3$ has the largest uncertainty grasp index. The other indices have the largest values in the grasp polygon $p_1p_{2e}p_3$.

Consequently, it is concluded that the grasp polygon $p_1p_{2c}p_3$ is selected as the optimal grasp polygon because this polygon imposes relatively large weighting factor on the uncertainty grasp index. Also, we can recognize that all grasp indices of the grasp polygon $p_1p_{2c}p_3$ are well-balanced in comparison to the others. Specifically, since the position of finger 2 is located at the nearest center of the feasible grasp region, it is natural to have the largest uncertainty grasp index in the grasp polygon $p_1p_{2c}p_3$. Table 3 also shows that there exists a trade-off between grasp indices. So, the proposed non-dimensionalized composite grasp index is useful when determining the optimal grasp by using task-based weighting factor.

Next, consider another peg-in-hole task of L-type object as shown in Figure 9. In this example, to find the optimal grasp positions for the given task, we analyze the optimal grasp positions according to the weighting factor. Particularly the feasible grasp region of finger 2 is limited because finger 2 is possible to collide with the under-edge of the hole.

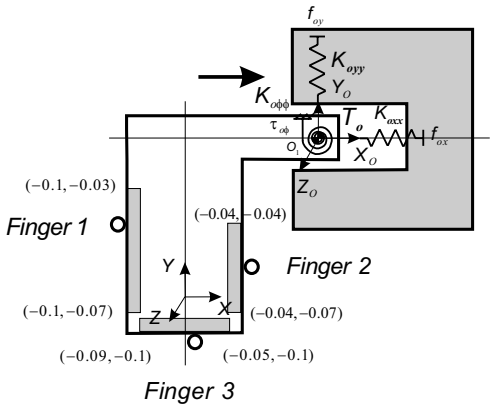

Figure 9: Peg-in-hole task with L-type object.

Table 4 illustrates the optimal grasp positions according to the specified weighting factor. In Table 4, x_j and y_j denote the x- and y-directional coordinates which represent the distances from the operational space to the fingertip space in Figure 9.

In Figure 9, the current grasp positions of the fingers represent the optimal grasp positions when employing the same weighting factors for all grasp indices. When the weighting factor for the stability grasp index is increased as 4.0, it is seen that the 3rd finger moves to the left-direction. Thus, the grasped geometry approaches to the shape of regular polygon. This represents more stable configuration. Also, we can observe that the 1st finger moves downward from the current grasp position if the weighting factor for the uncertainty grasp index is relatively large. Since the more a grasp position lies near the center of each feasible grasp region, the more the position sensitivity is insensible. Thus, this trend is natural.

Table 4: Optimal grasp positions by using the weighting factors

Weighting factors $w_i (i = 1, \cdots, 5)$	Grasp positions[m] j	$x_j,\ y_j$	I_{WCG}
1.0,1.0,1.0,1.0,1.0	1	$-0.1,\ -0.038$	0.6184
	2	$-0.04,\ -0.055$	
	3	$-0.066,\ -0.1$	
4.0,1.0,1.0,1.0,1.0	1	$-0.1,\ -0.038$	0.6105
	2	$-0.04,\ -0.055$	
	3	$-0.078,\ -0.1$	
1.0,4.0,1.0,1.0,1.0	1	$-0.1,\ -0.046$	0.4671
	2	$-0.04,\ -0.055$	
	3	$-0.066,\ -0.1$	
1.0,1.0,4.0,1.0,1.0	1	$-0.1,\ -0.03$	0.5058
	2	$-0.04,\ -0.055$	
	3	$-0.066,\ -0.1$	
1.0,1.0,1.0,4.0,1.0	1	$-0.1,\ -0.03$	0.4409
	2	$-0.04,\ -0.052$	
	3	$-0.062,\ -0.1$	
1.0,1.0,1.0,1.0,4.0	1	$-0.1,\ -0.03$	0.5059
	2	$-0.04,\ -0.055$	
	3	$-0.066,\ -0.1$	

On the other hand, to select the optimal grasp position with respect to the force transmission ratio or stiffness mapping-based grasp indices, we can recommend that the 1st finger should grasp the upper position from the current grasp position. In fact, this configuration is adequate to support large operational forces in the assembly task in comparison to the previous case. Also, we can obtain the optimal grasp

positions for considering the given task isotropy grasp index.

Through the analysis, it is concluded that we can effectively choose the desired grasp position for the given task by properly selecting the weighting factors. Consequently, to maintain strong uncertainty grasp configuration, it is desired that a multi-fingered hand should grasps the center position of each feasible grasp regions. Also, in the case of requiring large operational forces in the assembly task, it is necessary to assign a relatively large weighting for the force transmission ratio. However, selection of the weighting factors for the given tasks is still an open research problem.

4 Concluding Remarks

This paper proposes a new non-dimensionalized composite grasp index to choose the optimal grasp point in grasping and manipulation tasks using multi-fingered hands. Through the simulations for the two-dimensional assembly tasks using three-fingered hand, we illustrated the feasibility of the proposed generalized grasp index comparing to the physical sense of human grasping. The developed non-dimensionalized composite grasp index can be easily extended to consider some other indices and also can be applied to multiple robotic tasks. Continuously coordination of hands and arm and also development of kinematic indices associate with this problem will be future research area.

References

[1] Z. Li, P. Hsu, and S. Sastry, "Grasping and coordinated manipulation by a multi-fingered robot hand," *Int. Jour. of Robotics Research*, Vol. 8, No. 4, pp. 33-49, 1989.

[2] T. Yoshikawa and X. -Z. Zheng, "Coordinated dynamic hybrid position/force control for multiple robot manipulators handling one constrained object," *Int. Jour. of Robotics Research*, Vol. 12, No. 3, pp. 219-230, 1993.

[3] K. Nagai and T. Yoshikawa, "Grasping and manipulation by arm/multifingered-hand mechanisms," *Proc. of IEEE Int. Conf. on Robotics and Automation*, pp. 1040-1047, 1995.

[4] T. Hasegawa, T. Matsuoka, T. Kiriki, and K, Honda, "Manipulation of an object by a multi-fingered hand with multi-sensors," *Proc. of the Int. Conf. on Industrial Electronics, Control, and Instrumentation*, pp. 174-179, 1996.

[5] H. Maekawa, K. Tanie, and K. Komoria, "Dynamic grasping force control using tactile feedback for grasp of multifingered Hand," *Proc. of IEEE Int. Conf. on Robotics and Automation*, pp. 2462-2469, April 1996.

[6] Z. Li and S. Sastry, "Task oriented optimal grasping by multifingered robot hands," *Proc. of IEEE Int. Conf. on Robotics and Automation*, pp. 389-394, 1987.

[7] M. R. Cutkosky, "On grasp choice, grasp models, and the design of hands for manufacturing tasks," *Trans. on Robotics and Automation*, Vol. 5, No. 3, June 1989.

[8] Y. C. Park and G. P. Starr, "Optimal grasping using a multifingered robot hand," *Proc. of IEEE Int. Conf. on Robotics and Automation*, pp. 689-694, 1990.

[9] Y. C. Park and G. P. Starr, "Grasp synthesis of polygonal objects using three-fingered robot hand," *Int. Jour. of Robotics Research*, Vol. 11, No. 3, pp. 163-184, 1992.

[10] M. Kaneko and K. Tanie, "Contact point detection for grasping an unknown object using self-posture changeability," *IEEE Trans. on Robotics and Automation*, Vol. 10, No. 3, pp. 355-367, June 1994.

[11] J. -H. You, J. -H. Park, D. -H. Choi, and N. Y. Chong, "Optimal grasp design of a multi-fingered robot hand based on manipulability and stability," *Trans. of Korea Society of Mechanical Engineers (A)*, Vol. 22. No. 7. pp. 1367-1374, 1998.

[12] G. Strang, *Linear Algebra and Its Applications*, Harcourt Brace Jovanovich, Inc., 1988.

[13] B. -H. Kim, B. -J. Yi, I. H. Suh, and S. -R. Oh, "A biomimetic compliance control of robot hand by considering structures of human finger," *Proc. of IEEE Int. Conf. on Robotics and Automation*, pp. 3880-3887, 2000.

[14] T. Terano, K. Asai, and M. Sugeno, *Fuzzy Systems Theory and Its Applications*, Academic Press, Inc., Harcourt Brace Jovanovich, Publishers, 1992.

[15] K. L. Wood, *A method for the representation and manipulation of uncertainties in preliminary engineering design*, Ph. D. Dissertation, Dept. of Mechanical Eng., California Institute of Technology 1989.

[16] K. Stanley, J. Wu, A. Jerbi, and W. A. Gruver, "A fast two dimensional image based grasp planner," *Proc. of IEEE Int. Conf. on Intelligent Robots and Systems*, pp. 266-271, 1999.

[17] A. Hauck, J. Rttinger, M. Sorg, and G. Frber, "Visual determination of 3D grasping points on unknown objects with a binocular camera system," *Proc. of IEEE Int. Conf. on Intelligent Robots and Systems*, pp. 272-277, 1999.